

Proceedings of IMECE2002
ASME International Mechanical Engineering Congress & Exposition
November 17–22, 2002, New Orleans, Louisiana

IMECE2002-33219

THRESHOLD ENERGY SWITCHING AND ITS APPLICATION TO WIRELESS SENSING IN HIGH ENERGY MANUFACTURING PROCESSES

Charles B. Theurer /University of Massachusetts,
Amherst

David O. Kazmer / University of Massachusetts,
Lowell

Li Zhang / University of Massachusetts,
Amherst

Robert X. Gao / University of Massachusetts,
Amherst

ABSTRACT

A solid state threshold energy switching device based on a relaxation oscillator is discussed in the context of a self energizing wireless pressure sensor. The study is an integral part of the design of a wireless pressure sensor for in-situ injection molding machine cavity pressure measurement and real time process control. The pressure information is measured using a piezoelectric stack and converted to a train of ultrasonic pulses, using the oscillator based threshold switching device, to a receiver outside of the mold. In this paper the threshold switching device is developed, simulated using a circuit simulation program, and validated experimentally. Its properties are discussed with reference to pressure measurement and acoustic signal transmission.

INTRODUCTION

It has been shown that direct cavity pressure and temperature measurement, more than any indirect method, is related to final part quality [1-3]. For this reason the development of a low cost, reliable cavity pressure measurement system has been the subject of this research. A typical cavity pressure sensor in an injection mold consists of a measurement diaphragm connected by a capillary tube to another measurement diaphragm that is remote to the process where the information is translated from a mechanical signal to an electrical signal. Because of the complexity of most injection molds, the cost to install such a device can be on the order of the cost of the sensor itself. The majority of the installation cost is associated with cabling or providing a pathway for the information to travel from the sensor to the process controller. The proposed self energized wireless sensor would be installed in the cavity of the injection mold, extract energy from the injection pressure, and send the pressure information in the form of a train of ultrasonic pulses through the mold steel to an acoustic receiver located outside the mold.

Such a wireless pressure sensor makes it economically possible to have multiple sensors per cavity or a sensor in each cavity of a multi-cavity mold (Fig. 1.)

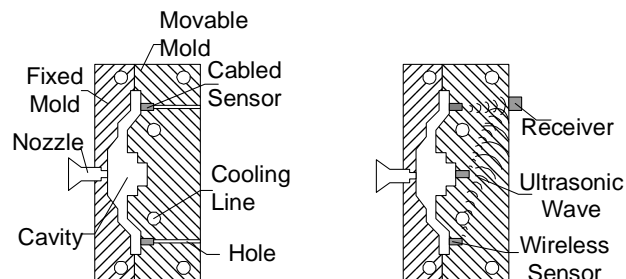


Fig. 1. Existing cabled cavity pressure sensor (left) and remote cavity pressure sensor (right)

It has been proposed that the implementation of a wireless molding pressure sensor consists of two structures [4]: a remote sensing-transmitting structure and a receiver structure. The remote sensor generates an electrical signal as a result of a change in pressure. A pressure change in the mold produces a sequence of electrical pulses, each representing a finite change in pressure. This digital signal is converted to an acoustic signal through the use of a secondary piezoelectric element. The receiving unit detects the acoustic pulses and demodulates the signal in order to estimate the pressure in the mold cavity. This paper is largely concerned with the development and simulation of the energy collector and threshold modulator in the remote sensing unit, which is required to encode the pressure information and convert the energy to the form of an electric pulse (highlighted in Fig. 2).

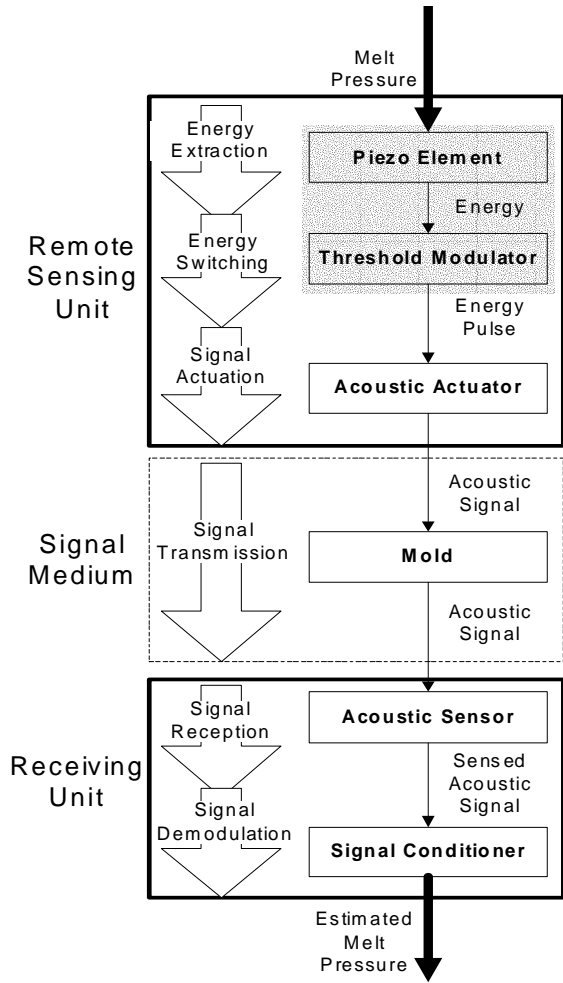


Fig. 2 System diagram of a remote cavity pressure sensor

ENERGY EXTRACTION

Piezoelectric elements generate a charge when stress is applied. This charge is associated with the deformation of the polarized molecules in the crystal structure [5-7]. If electrodes are placed on opposite sides of the element, the charge can be collected and used. The energy stored in the element is stored in two forms; 1) electrically in the form of an electric field and, 2) mechanically in the form of strain [8]. The interaction between the strain and the electric field is the subject of the model presented next. A stack of N piezoelectric rings is used to extract energy from the pressure in the injection mold (Fig. 3). In order to evaluate the threshold switch an analytical representation of the sensing element is derived and applied to an electrical circuit representation.

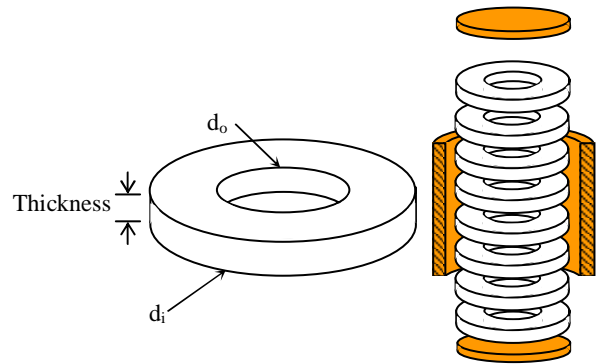


Fig. 3. Schematic representation of piezoelectric stack prototype

The current produced by the stack can be calculated from the definition of current [9]:

$$I = \frac{dq}{dt} \quad (1)$$

where dq is the charge accumulated on the electrodes in the stack and dt is the total time associated with the pressure ramp. The charge accumulated can also be expressed in terms of the capacitance, C , of the stack and the voltage, V , generated by the applied stress:

$$dq = C \cdot V. \quad (2)$$

The total capacitance of the piezoelectric stack can be approximated by the sum of the capacitance of the individual parallel plates [10]:

$$C = \frac{1}{h} (\epsilon_0 \cdot \epsilon_r \cdot A_{cr}) N \quad (3)$$

where h is the thickness, ϵ_0 is the permittivity of free space, ϵ_r is the relative permittivity of the piezoelectric material, A_{cr} is the area of the piezoelectric disk (not including the center hole) and N is the total number of disks in the stack. A_{cr} can be expressed in terms of the inner diameter and the outer diameter as:

$$A_{cr} = \frac{\pi}{4} (d_o^2 - d_i^2) \quad (4)$$

The voltage in Equation 2 can be expressed in terms of the materials piezoelectric charge constant (g_{33}) and the change in stress in the material as a result of the pressure differential (dT):

$$V = g_{33} \cdot h \cdot dT \quad (5)$$

The change in stress is a function of the area of the crystal and the force applied (dF):

$$dT = \frac{dF}{A_{cr}} \quad (6)$$

The area of the crystal (A_{cr}) is defined in Equation 4, however the force (dF) is a function of the change in pressure and the total sensor footprint over which the pressure is acting (A_{fp}):

$$A_{fp} = \frac{1}{4}(\pi \cdot d_o^2) \quad (7).$$

For reasons that will be discussed later, it is convenient to represent time associated with the pressure rise (from Equation 1) in terms of the pressure ramp rate (rr):

$$dt = \frac{dP}{rr} \quad (8).$$

Substituting Equations 2-8 into Equation 1 yields an expression for the current produced by the stack in terms of material, geometric, and loading parameters:

$$I = \frac{1}{4} \cdot \pi \cdot rr \cdot d_o^2 \cdot g_{33} \cdot \epsilon_o \cdot \epsilon_r \quad (9).$$

The piezoelectric stack can now be modeled as an electric circuit consisting of a current source described in Equation 9 in parallel with a capacitor described in Equation 3 (Fig. 4).

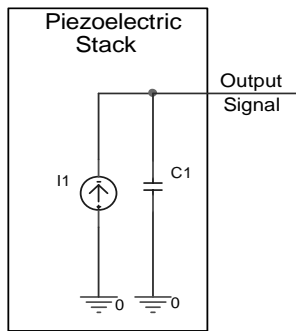


Fig. 4. Circuit Simulation of a piezoelectric stack under a pressure-ramp load

The current I at any point in time is directly proportional to the pressure ramp rate while the capacitance $C1$ can be calculated from the stack parameters. Experimental evidence has shown a very good correlation between the calculation of the two simulation parameters and their actual values. [11]

ENERGY SWITCHING

The charge will continue to accumulate on the stack electrodes producing a voltage potential. Once this voltage reaches a predetermined threshold the energy associated with the charge at this voltage level is used to power an acoustic transmitter that will transmit the pressure information out of the mold [11].

Signal Discretization:

The resolution of any threshold sensor can be controlled by the amount of energy required to change the state of the

switching element. However, a certain amount of energy will be required to send an acoustic signal through the mold to the receiver. The energy required to send a detectable acoustic pulse to the outside of the mold depends many factors and is the subject of parallel research. A brief overview of these factors can be found in [11]. Therefore the resolution of any threshold sensor will depend on the amount of energy required to produce a detectable signal.

The energy requirements of the sensor place a constraint on the number of pulses the sensor can emit during a single molding cycle and consequently there is a constraint on sensor resolution. However, a discrete signal (pulse) emitted from the sensor would transmit less information and therefore need less power when compared with a continuous acoustic signal. As shown in Fig. 5, this approach generates a modulated approximation of the continuous pressure trace; a close approximation of the pressure curve can be obtained with relatively few acoustic pulses. For this example the continuous signal required a minimum of 160 units of energy (8 bits * 20 signals), compared to the discrete signal requiring only 10 units of energy (2 bits * 5 signals).

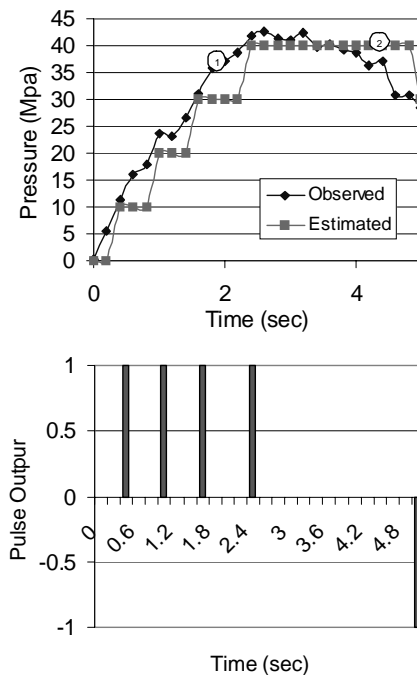


Fig. 5. Continuous (1) vs. discrete (2) sampling of pressure and associated pulse output

Threshold Switch:

It is now useful to consider the threshold switching element itself. An ideal threshold switch should present infinite resistance off state when the voltage on the

piezoelectric stack is below some threshold level (Fig. 6 A to B) and minimized resistance on state when the voltage on that stack is at or above that level (Fig. 6 C). As the charge is used, the current decreases rapidly (Fig. 6 C to D). Once the charge on the stack is exhausted the ideal switch would then revert to an off state (Fig. 6 D). The charge would again begin to accumulate and the state of the switch would repeat the loop D-B-C as long as the pressure on the piezoelectric stack continues to increase.

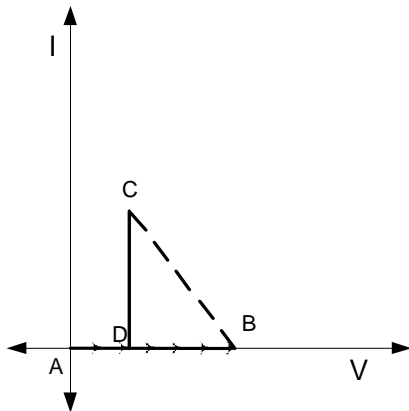


Fig. 6. V-I curve for ideal threshold switch

The V-I curve in Fig. 6 can be modeled and designed as a relaxation oscillator shown in Fig. 7. This device consists of PNP (Q1) and NPN (Q2) transistors connected such that the gate of the first is connected to the emitter of the second and the gate of the second is connected to the emitter of the first. Because the transistors have a finite off resistance, some current passes through Q1 as the input signal voltage rises, which causes Q2 to be triggered which in turn causes Q1 to trigger. At this point, the switch represented in the figure by Q1, Q2 and R2 changes from the relative off state to the on state (B to C). The capacitor C2 is then discharged through the output signal, in the form of a pulse, until there is no longer enough current to maintain the on states of the two transistors. The switch then changes to the off state (D) and the cycle can be repeated as long as there is current supplied at the input signal.

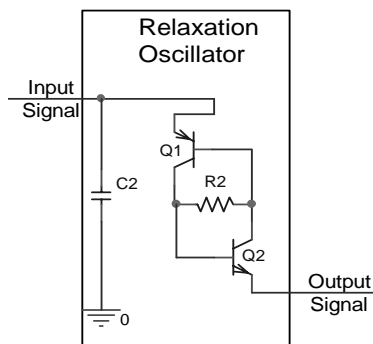


Fig. 7. Threshold switch based on a relaxation oscillator

A simulation of the above threshold switch produced the V-I curve presented in Fig. 8. It is important to note that the switch doesn't snap back in the simulation because an ideal voltage source with infinite impedance is used to trace the curve. In a device with a finite impedance, the current increase from B to C the would reduced the voltage and the V-I curve would more closely match the ideal curve described in Fig. 6.

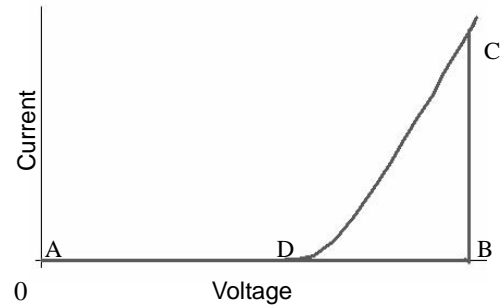


Fig. 8. V-I Curve for threshold switch based on a relaxation oscillator

As the approximation of the piezoelectric stack, described in Fig. 4, and a load resistor are connected to the threshold switch being evaluated, the resulting electrical model is an approximation of the piezoelectric pressure sensor (Fig. 9).

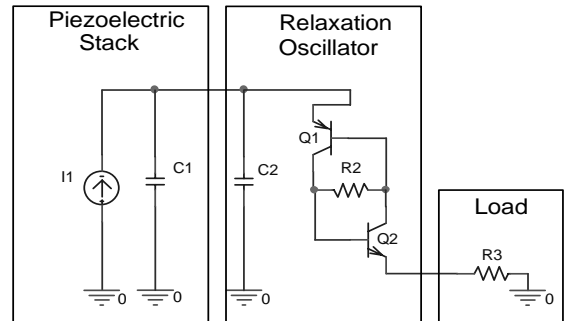


Fig. 9. Electric circuit model of a threshold pressure sensor

The circuit in Fig. 9 can be modeled and simulated. When a DC current is used as the current source $I1$, the piezoelectric stack effectively simulates a linear pressure ramp and the circuit responds as described in Fig. 10. The sensor model produces a series of pulses in response to a simulated linear pressure ramp. The number of pulses produced is proportional to the pressure exerted on the sensor minus some activation pressure. This is consistent with the signal discretization schema discussed earlier and presented in Fig. 5.

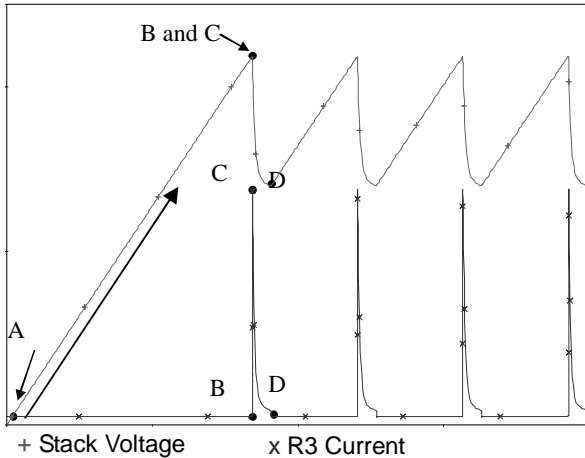


Fig. 10 Response of threshold pressure sensor model to a ramped pressure input

| Experimental Stack Constants | | | |
|------------------------------|----------|-----------|----------|
| Name | Symbol | Value | Units |
| Height (ring thickness) | h | 1.000E-03 | m |
| Outer diameter | d_o | 1.000E-03 | m |
| Inner diameter | d_i | 1.000E-02 | m |
| Number of rings | Num | 1.000E+01 | (none) |
| Ramp Rate | rr | 1.000E+09 | Pa/s |
| Pressure | dP | 1.000E+08 | Pa |
| Current | I1 | 3.041E-04 | A |
| Capacitance | C1 | 1.204E-08 | F |
| Stack Current Constant | α | 3.041E-13 | A/(Pa/s) |

The complete circuit model including nominal values for each of the circuit elements is presented in Fig. 11. The capacitor C1 represents the actual capacitance of the piezoelectric stack calculated using Equation 3. The transistor models Q1 and Q2 are general-purpose transistors for switching and amplifier applications manufactured by Semicoa™ and Fairchild Semiconductor™ respectively. The remainder of the circuit elements C2, R2 and R3 were nominal values that produce a pulsed output at R3.

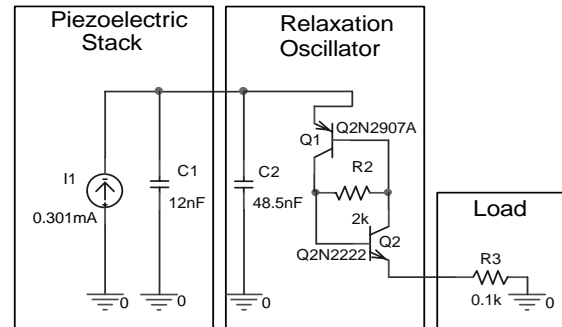


Fig. 11. Electric circuit model of a threshold pressure sensor

A prototype of the above circuit was built using a Keithley 2400 source meter in place of the ideal current source. Due to availability, the PNP transistor used in the simulation was replaced with a Fairchild 2N3906 PNP general purpose amplifier transistor. Likewise the NPN transistor was replaced with a Fairchild 2N3904 NPN general purpose amplifier. This replacement made little difference in the low power dynamic response of the system. The voltages in the circuit was measured using a Tektronix 3012 100 M Ω digital oscilloscope. The input and output voltages were measured between the emitter of Q1 to ground and the emitter of Q2 to ground respectively. The output current was calculated using Ohm's law

The experimental and simulation results of a transient analysis of the specific model given in Fig. 11 are presented below. Fig. 12 shows the stack voltage and current output for the model with a pressure ramp rate given in

Table 1 as 1E8 Pa/sec. Each current pulse represents a pressure change of 10.8 kPa for every output pulse, corresponding to 0.001% of a possible 100 MPa pressure range (12 bit accuracy). The current source was switched on at time

RESULTS

A simulation of the circuit in Fig. 9 was performed using the constants and boundary conditions associated with a piezoelectric disk available from American Piezo-Ceramic. The electrical and geometric constants associated with the piezoelectric stack that was simulated are presented in Table 1.

Table 1
Electric and conditions associated with the simulated piezoelectric stack

| APC 850 Constants | | | |
|----------------------------|--------------|-----------|-------|
| Name | Symbol | Value | Units |
| Charge constant | g_{33} | 2.500E-02 | C/N |
| Permittivity of free space | ϵ_o | 8.850E-12 | F/m |
| Relative permittivity | ϵ_r | 1.750E+03 | 1 |

It is possible to calculate the electrical parameters, $I1$ and $C1$, associated with the circuit simulation of the piezoelectric stack in Fig. 4. It is also possible to calculate the proportionality constant that describes the relationship between pressure ramp rate (rr) and the current ($I1$). These parameters as well as the boundary conditions are presented in Table 2.

Table 2
Experimentally obtained Electric, geometric and boundary conditions associated with the simulated piezoelectric stack

= 0 and the circuit began stable oscillation after reaching the switch breakdown voltage.

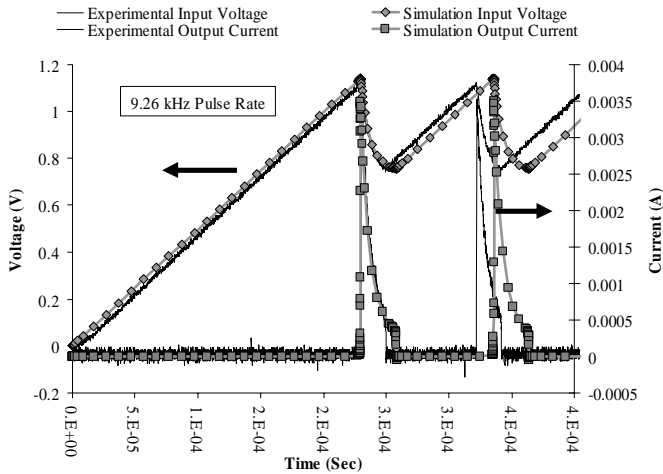


Fig. 12. Transient (startup) experimental and simulation results for a threshold pressure sensor

The magnitude of the experimental results matched very closely that of the simulation. The total pulse width varies by about 25%. This appears to be from a difference in holding current between the transistors used in the simulation and those used in the experiment Fig. 13. Otherwise, however, the experimental results closely matched those predicted. The output pulse width shown is approximately 30µs. This pulse width corresponds to a 33kHz (tip to tail) maximum repetition frequency.

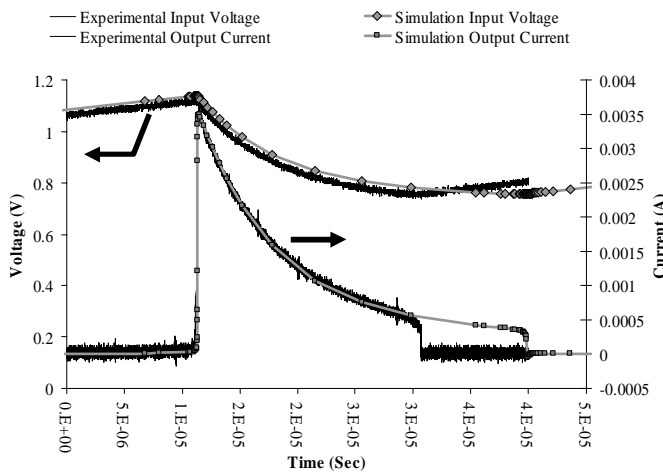


Fig. 13. Experimental and simulation results: Output pulse current and corresponding input voltage for a threshold pressure sensor

Fig. 14 shows the output pulse leading edge. The corresponding rise time is approximately 40 ns; this rise time represents a maximum excitation frequency of 12.5 MHz.

This means that the output pulse if directly connected to an acoustic transmitter would be able to excite a 12.5 MHz mode of vibration. This is well above the proposed operating frequency of an acoustic transmitter designed for acoustic telemetry in injection molding [12].

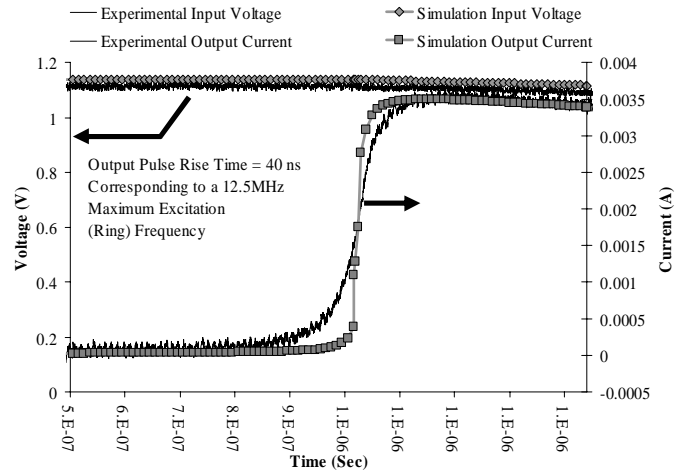


Fig. 14. Electric circuit model of a threshold pressure sensor

The threshold switch is stable only between two current limits. Below its lower limit the current cannot reach the switch's required on voltage, and above its upper limit the current never goes below the switches holding current. These limits are the reason for including the parallel resistor R2. By adjusting the resistance of this element it is possible to change the characteristics associated with the switch.

Table 3 shows the results of current sweep from 0 to 0.4 Amps. The stable ramp rates associated with the nominal value of 2 kΩ for R2 are between 9.87E4 MPa/sec and 1.24E6 MPa/sec. Ramp rates outside of this limit will not produce output pulses. While the upper limit on ramp rate far exceeds the capability of actual manufacturing processes, further design refinement is required to operate at lower ramp values.

Table 3
Simulation and experimentally determined limits associated with the threshold switch

| | Simulation Lower Stable Limit | Simulation Upper Stable Limit | Experimental Lower Stable Limit | Experimental Upper Stable Limit |
|-------------------|-------------------------------|-------------------------------|---------------------------------|---------------------------------|
| Current (A) | 3.000E-05 | 3.780E-04 | 3.995E-05 | 4.61E-04 |
| Ramp Rate (Pa/s) | 9.865E+07 | 1.243E+09 | 1.314E+08 | 1.516E+09 |
| Ramp Rate (PSI/s) | 1.431E+04 | 1.803E+05 | 1.905E+04 | 2.199E+05 |
| Frequency (kHz) | 1.192 | 10.932 | 1.608 | 13.91 |

CONCLUSION

Several fundamental aspects related to the design of a new type of wireless acoustic sensor for injection molding cavity pressure measurement were introduced. The sensor will measure the change of pressure by means of a train of ultrasonic pulses. A stack of piezoceramic disks in the mold cavity are used to extract energy from the pressure differential in the mold cavity. This energy is switched upon reaching a predetermined threshold and used to produce an acoustic pulse that can be detected wirelessly outside of the mold cavity. An electrical circuit representation of the piezoelectric stack and threshold switch are developed and simulated. The results of the simulation are presented with recommendations for the development of a threshold pressure sensor. Further numerical simulation and experimental studies are being conducted for the prototyping of a wireless pressure measurement system.

ACKNOWLEDGMENTS

The authors gratefully acknowledge funding provided to this research by the National Science Foundation under award DMI-9988757.

REFERENCES

- [1] I. A. Rawabdeh and P. F. Petersen, "In-Line Monitoring of Injection Molding Operations: A Literature Review," *Injection Molding Technology*, vol. 3, pp. 47-53, 1999.
- [2] B. Watkins, "Five Myths about Sensing Mold Pressure," in *Sensors Magazine*, vol. 14, 1997, pp. 73-78.
- [3] Federico Manero, W. I. Patterson, and Musa R. Kamal, "Cavity temperature profile measurement during injection moulding," presented at Annual Technical Conference - ANTEC, Conference Proceedings, 1997.
- [4] C. Theurer, "Investigation Of A Remote Pressure Sensor For Real Time Control Of An Injection Molding Machine," in *Mechanical and Industrial Engineering*. Amherst: University of Massachusetts, 2001, pp. 68.
- [5] Channel Industries, "Piezoelectric Ceramics Equations," vol. 2001, 2001.
- [6] J. Van Randeraat and R. E. Settingington, *Piezoelectric ceramics*, 2d ed. London: Mullard, 1974.
- [7] Devdas Shetty and Richard Kolk, *Mechatronics system design*. Boston: PWS Pub., 1997.
- [8] Won-kyu Moon and Ilene J. Busch-Vishniac, "Modeling of piezoelectric ceramic vibrators including thermal effects. Part II. Derivation of partial differential equations," *The Journal of the Acoustical Society of America*, vol. 98, pp. 413-421, 1995.
- [9] Leonard S. Bobrow, *Fundamentals of electrical engineering*. New York: Holt Rinehart and Winston, 1985.
- [10] J. W. Waanders, *Piezoelectric Ceramics Properties and Applications*. Eindhoven: Philips, 1991.
- [11] L. Zhang, C. Theurer, R. Gao, and D. Kazmer, "Design of a wireless sensor for injection molding cavity pressure measurement," presented at ASME International Mechanical Engineering Congress and Exhibition, New York, NY, 2001.
- [12] C. Theurer, L. Zhang, R. Gao, and D. Kazmer, "Acoustic telemetry in injection molding," presented at Process Monitoring And Control Division, Society of Plastics Engineers Annual Technical Conference, Dallas, TX, 2001.